

9-4-2000

Sm–Co–Cu–Ti high-temperature permanent magnets

Jian Zhou

University of Nebraska - Lincoln

Ralph Skomski

University of Nebraska-Lincoln, rskomski2@unl.edu

C. Chen

Electron Energy Corporation, Landisville, Pennsylvania

George C. Hadjipanayis

University of Delaware, hadji@udel.edu

David J. Sellmyer

University of Nebraska-Lincoln, dsellmyer@unl.edu

Follow this and additional works at: <http://digitalcommons.unl.edu/physicsellmyer>



Part of the [Physics Commons](#)

Zhou, Jian; Skomski, Ralph; Chen, C.; Hadjipanayis, George C.; and Sellmyer, David J., "Sm–Co–Cu–Ti high-temperature permanent magnets" (2000). *David Sellmyer Publications*. 57.

<http://digitalcommons.unl.edu/physicsellmyer/57>

This Article is brought to you for free and open access by the Research Papers in Physics and Astronomy at DigitalCommons@University of Nebraska - Lincoln. It has been accepted for inclusion in David Sellmyer Publications by an authorized administrator of DigitalCommons@University of Nebraska - Lincoln.

Sm–Co–Cu–Ti high-temperature permanent magnets

J. Zhou and R. Skomski

*Department of Physics and Astronomy and Center for Materials Research and Analysis,
University of Nebraska, Lincoln, Nebraska 68588*

C. Chen

Electron Energy Corporation, Landisville, Pennsylvania 17538

G. C. Hadjipanayis

Department of Physics and Astronomy, University of Delaware, Newark, Delaware 19716

D. J. Sellmyer^{a)}

*Department of Physics and Astronomy and Center for Materials Research and Analysis,
University of Nebraska, Lincoln, Nebraska 68588*

(Received 19 April 2000; accepted for publication 11 July 2000)

A class of promising permanent-magnet materials with an appreciable high-temperature coercivity of 8.6 kOe at 500 °C is reported. The Sm–Co–Cu–Ti magnets are prepared by arc melting and require a suitable heat treatment. Magnetization measurements as a function of temperature and x-ray diffraction patterns indicate that the samples are two-phase mixtures of 2:17 and 1:5 structures. Depending on heat treatment and composition, some of the magnets exhibit a positive temperature coefficient of coercivity. The promising high-temperature behavior of the coercivity is ascribed to the temperature dependence of the domain-wall energy, which affects the curvature of the walls and the pinning behavior. © 2000 American Institute of Physics.

[S0003-6951(00)02836-9]

Permanent magnets for high-temperature applications are a research area of great scientific and industrial interest. While the best room-temperature permanent magnets are now made from Nd₂Fe₁₄B,^{1,2} Sm–Co magnets have retained their dominance at elevated temperatures.^{2–10} The reason is the strong interatomic exchange between the Co atoms, which gives rise to a high Curie temperature and ensures a high anisotropy in the temperature region of interest, which is above 450 °C.^{2,11} Most high-temperature permanent magnets are Sm₂Co₁₇–SmCo₅ two-phase magnets characterized by a cellular microstructure and pinning-controlled coercivity,^{4–8,12,13} and at 500 °C coercivities of up to 10 kOe have been obtained in optimized magnets.⁷ Other approaches involve additives such as Mn¹⁴ to improve the overall performance of the material.

Here we report a Ti-substituted material exhibiting interesting hysteretic properties at high temperatures and discuss the observed behavior in terms of domain-wall energies.

The starting material, namely as-cast samples with the nominal composition Sm(Co_xCu_{0.6}Ti_y) (x = 6.1–6.7, y = 0.25 and 0.3) were prepared by arc melting. The as-cast alloys crystallize in the disordered 1:5 phase, which is commonly referred to as the TbCu₇ (or 1:7) phase. The 1:7 structure does not correspond to a periodic crystal—the simplest conceivable dumbbell-substituted compound with a 1:7 composition is Sm₇Co₄₉, corresponding to a stacking of two Sm₂Co₁₇ and three SmCo₅ unit cells—but for simplicity we will keep the popular notation Sm(Co, Cu, Ti)₇.

Some samples were annealed at 1150 °C for 2 h and then cooled down (method I). Others were annealed first at 1185 °C for 3 h, then annealed at 850 °C for 8 h, and finally subjected to slow cooling at 1 K/min from 850 to 600 °C

(method II). Figure 1 shows the X-ray diffraction patterns (a) before and (b) after annealing. From the x-ray data we see that the 1:7 phase segregates into two phases: a nearly stoichiometric 1:5 grain-boundary phase, crystallizing in the CaCu₅ structure, and a main 2:17 phase, very likely having the rhombohedral Th₂Zn₁₇ structure. In particular, the (204) peak is characteristic of the 2:17 phase but absent in the 1:5 and 1:7 phases. The two-phase character of the material is confirmed by thermomagnetic analysis (Fig. 2).

The microstructure of the material was investigated by transmission electron microscopy (TEM), energy-dispersive x-ray spectroscopy (EDX), and high-resolution transmission

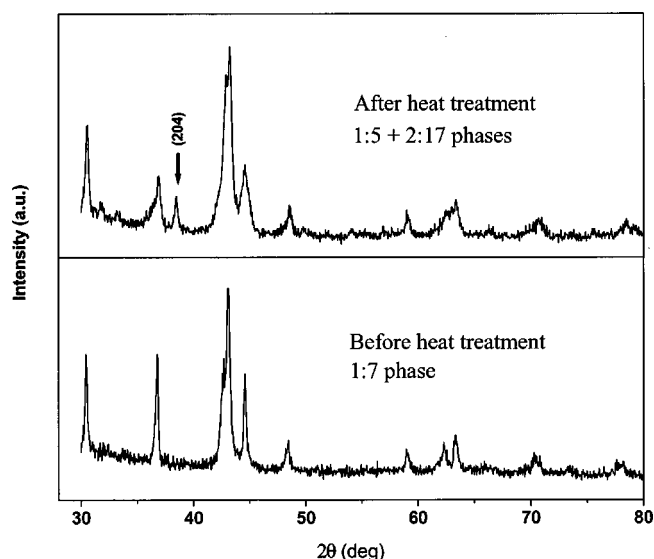


FIG. 1. X-ray diffraction pattern (a) before and (b) after annealing. The arrow shows a characteristic 2:17 peak.

^{a)}Electronic mail: cmra@unlinfo.unl.edu

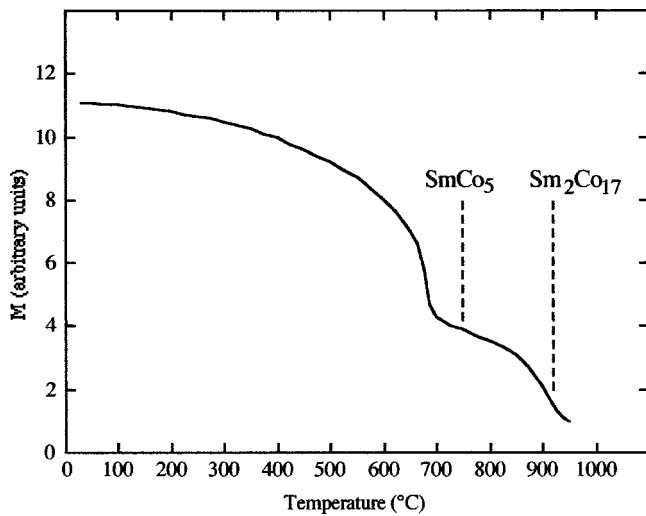


FIG. 2. Thermomagnetic analysis of $\text{SmCo}_{6.1}\text{Cu}_{0.6}\text{Ti}_{0.3}$ magnet. The dashed lines show the Curie temperatures of the pure $\text{Sm}_2\text{Co}_{17}$ and SmCo_5 phases.

electron microscopy (HRTEM). Figure 3 shows a bright-field image of the $\text{SmCo}_{6.7}\text{Cu}_{0.6}\text{Ti}_{0.3}$ sample annealed at 1150°C for 2 h. The microstructure is cellular and reminiscent of that of industrial 2:17 magnets. EDX and HRTEM were used to characterize the cellular 2:17 and 1:5 grain-boundary phases. EDX reveals that the grain-boundary phase contains more Cu than the 2:17 cells, and HRTEM shows that the grain-boundary and cellular phases are coherent.

Figure 4 shows typical hysteresis loops. The field range was limited by our maximum field of 10 kOe, but measurements up to 18 kOe did not yield any further increase in H_c . The virgin curves—compare the 250°C loop in Fig. 4—exhibit features of domain-wall pinning, and the single-phase character of the loops speaks against a noninteracting mixture of weakly textured or isotropic 2:17 and 1:5 crystallites. No attempts have been made to produce aligned magnets, so that the remanence ratio M_r/M_s is significantly smaller than one, and the energy product, about 4 MJ Oe at 500°C , is only moderate.

The temperature dependence of the coercivity of typical Sm–Co–Cu–Ti high-temperature permanent magnets is

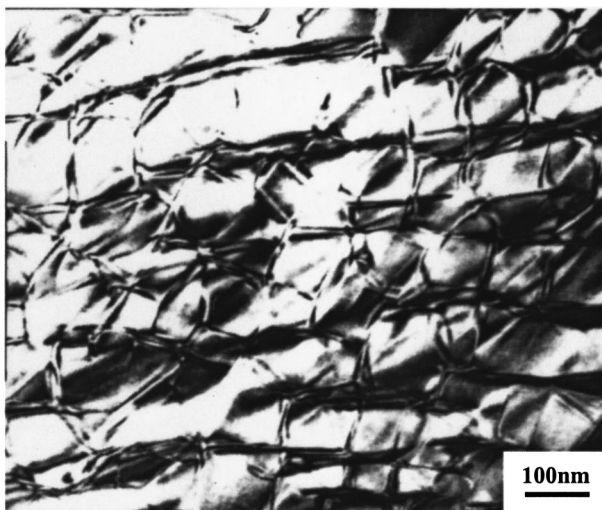


FIG. 3. TEM micrograph showing the microstructure of $\text{Sm}(\text{Co}_{6.7}\text{Cu}_{0.6}\text{Ti}_{0.3})$ magnet.

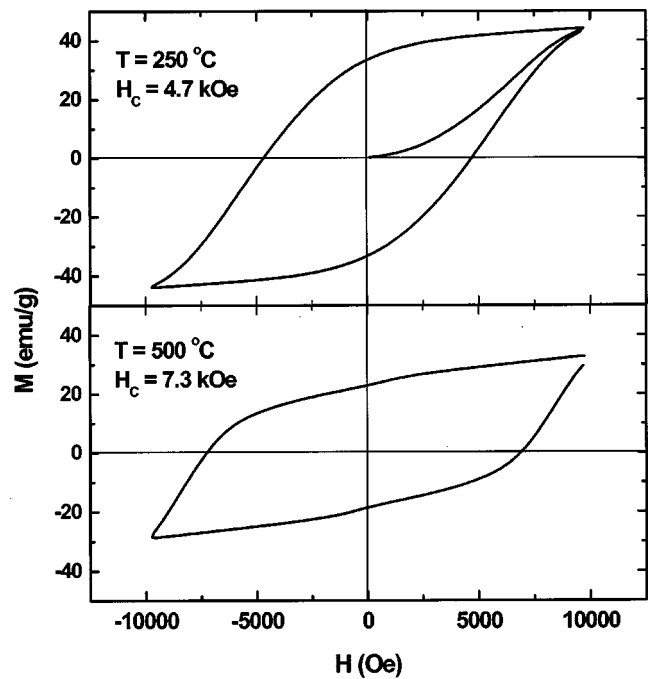


FIG. 4. Hysteresis loops of $\text{Sm}(\text{Co}_{6.1}\text{Cu}_{0.6}\text{Ti}_{0.3})$ at two elevated temperatures.

shown in Fig. 5. To exclude the possibility of structural aging, we have heated the material from room temperature to 550°C and then cooled back to room temperature; no change in coercivity was observed. The three samples shown in Fig. 5 exhibit positive temperature coefficients dH_c/dT up to about $400\text{--}500^\circ\text{C}$. The best coercivity, 8.6 kOe at 500°C , was obtained for a $\text{Sm}(\text{Co}_{6.4}\text{Cu}_{0.6}\text{Ti}_{0.3})$ sample produced by the heat-treatment method II. By comparison, the other two samples were heat-treated by method I. Other compositions lead to different temperature dependences (not shown in Fig. 5). For example, $\text{Sm}(\text{Co}_{6.15}\text{Cu}_{0.6}\text{Ti}_{0.25})$ exhibits a temperature coefficient dH_c/dT close to zero over a wide range of temperatures.

The temperature dependence of extrinsic properties,

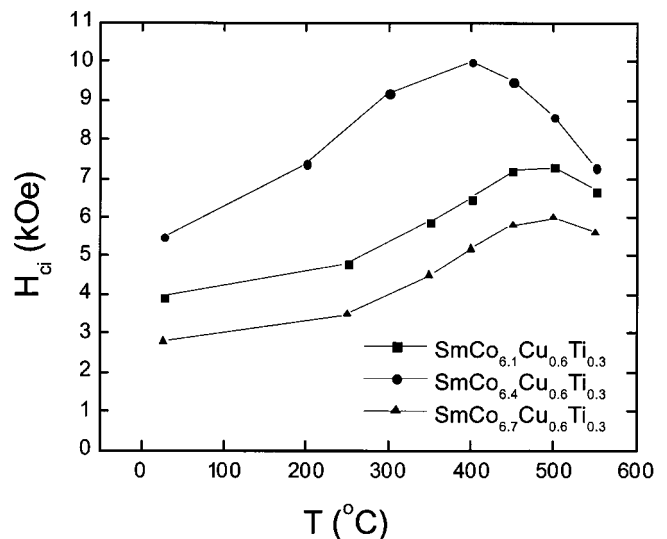


FIG. 5. Temperature dependence of the coercivity for three Sm–Co–Cu–Ti samples.

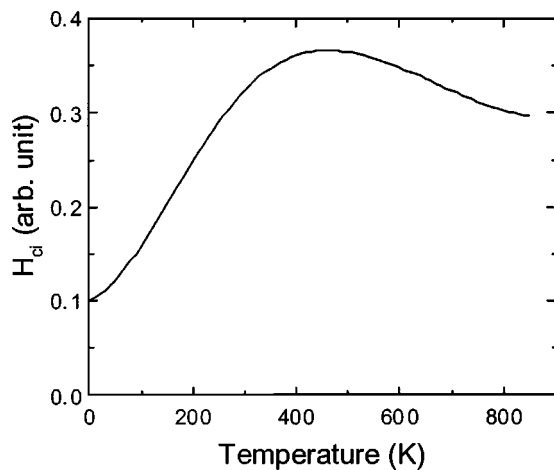


FIG. 6. Model calculation of the temperature dependence of the pinning coercivity.

such as coercivity, is largely given by the temperature dependence of the underlying intrinsic properties.^{2,11} By contrast, micromagnetic thermal excitations (magnetic-viscosity corrections) are unable to realize magnetization reversal without the help of energy-barrier reducing fields.¹⁵

Of key importance is the temperature dependence of micromagnetic parameters such as domain-wall energy $\gamma = 4\sqrt{AK_1}$ and thickness $\delta = \pi\sqrt{A/K_1}$ of the phases involved, where A and K_1 are the exchange stiffness and the first anisotropy constant, respectively.^{2,16} For the present material, the temperature dependences of the 1:5 and 2:17 anisotropies are not known, and even in the case of industrial 2:17 magnets there remain open questions. It is, however, instructive to discuss some conceivable mechanisms.

When the wall energy of the two phases is different, then the 2:17 domain walls may be trapped in 1:5 regions ($\gamma_{1:5} < \gamma_{2:17}$, attractive pinning) or unable to enter the 1:5 regions ($\gamma_{1:5} > \gamma_{2:17}$, repulsive pinning). Here we make the crude assumption that the coercivity is proportional to the difference between the first anisotropy constants of the two phases. From the general behavior of the temperature dependence of the anisotropy^{2,11} then follows the qualitative behavior shown in Fig. 6. However, a quantitative determination of the peak height and its position requires a detailed knowledge of the main and grain-boundary phases.

On the other hand, as discussed in Ref. 13, the domain-wall energy of the 2:17 phase determines the curvature of the domain walls and affects the coercivity by more or less exploiting the pinning potential of the 1:5 regions. The radius of curvature is given by $R = \gamma/\mu_0 M_s H_c$, and taking $\mu_0 M_s = 1.1$ T, $K_1 = 2$ MJ/m³, $A = 20$ pJ/m, and $\mu_0 H_c = 0.7$ T (7 kOe) we obtain the typical value $R = 41$ nm. This radius is well in the range of the structural features of the cellular composites in question.

A new aspect of the effect of the domain-wall curvature on the coercivity is its temperature dependence. For cell sizes much larger than the radius of curvature, the wall may be accommodated at almost any temperature, and the intrinsic dependence $dK_1/dT < 0$ is the key consideration, yielding $dH_c/dT < 0$. For small cell sizes, the wall-curvature radius may be larger than the cell size, and only a small “weak-pinning” fraction of the 1:5 phase contributes to the pinning.

This amounts to a comparatively small coercivity at low temperature. On heating, K_1 and γ become smaller, the wall curvature increases, and the enhanced pinning overcompensates the K_1 reduction in some intermediate temperature region ($dH_c/dT > 0$).

Note that another approach⁵ ascribes the observed behavior to micromagnetic fluctuations (magnetic viscosity). In Ref. 6, the earlier-mentioned intrinsic temperature dependence has been taken into account, but that magnetic-viscosity approach leads to the physically unreasonable result that $H_c = \infty$ for $T = 0$.

A key feature of the present materials is the absence of Zr, which helps to develop the cellular microstructure necessary to create coercivity in conventional Sm–Co magnets.^{2,3,13} In fact, Fig. 3 shows that Zr is not necessary to create a cellular microstructure. Note also that, compared to industrial Sm–Co magnets, the magnets are comparatively Sm rich, corresponding to a fairly large volume fraction of the 1:5 phase and the amount of the Ti (about 0.04 Ti atoms per Co atom) is roughly two times larger than that of zirconium in conventional high temperature magnets.

In conclusion, we have reported a 2:17–1:5 Sm–Co–Cu–Ti permanent magnet material with promising high-temperature properties. For the nominal composition Sm(Co_{6.4}Cu_{0.6}Ti_{0.3}), a positive temperature coefficient dH_c/dT and a coercivity of 8.6 kOe at 500 °C have been obtained. The temperature dependence of the coercivity reflects the microstructure of the two-phase magnet and is discussed in terms of the dependence of anisotropy and domain-wall curvature on temperature. However, since neither the exact microchemistry nor the effect of the Ti on the intrinsic properties of the material are known, a detailed description of the coercivity remains a challenge.

The authors are grateful to J. P. Liu, S. Liu, Y. Liu, and H. Tang for the discussion of various experimental aspects. This research is supported by AFOSR, DARPA/ARO, and DOE.

¹M. Sagawa, S. Fujimura, H. Yamamoto, and Y. Matsuura, *IEEE Trans. Magn.* **20**, 1584 (1984).

²R. Skomski and J. M. D. Coey, *Permanent Magnetism* (Institute of Physics, Bristol 1999).

³K. Kumar, *J. Appl. Phys.* **63**, R13 (1988).

⁴C. H. Chen, M. S. Walmer, M. H. Walmer, S. Liu, E. Kuhl, and G. Simon, *J. Appl. Phys.* **83**, 6706 (1998).

⁵J. F. Liu, T. Chui, D. Dimitrov, and G. C. Hadjipanayis, *Appl. Phys. Lett.* **73**, 3007 (1999).

⁶S. Liu, J. Yang, G. Doyle, G. Potts, and G. E. Kuhl, *J. Appl. Phys.* **87**, 6728 (2000).

⁷J. F. Liu, Y. Zhang, D. Dimitrov, and G. C. Hadjipanayis, *J. Appl. Phys.* **85**, 2800 (1999).

⁸J. F. Liu, Y. Ding, Y. Zhang, D. Dimitar, F. Zhang, and G. C. Hadjipanayis, *J. Appl. Phys.* **85**, 5660 (1999).

⁹T. Schrefl, J. Fidler, and W. Scholz, *IEEE Trans. Magn.* (to be published).

¹⁰G. C. Hadjipanayis, W. Tang, Y. Zhang, S. T. Chui, J. F. Liu, C. Chen, and H. Kronmüller, *IEEE Trans. Magn.* (to be published).

¹¹R. Skomski, *J. Appl. Phys.* **83**, 6724 (1998).

¹²G. C. Hadjipanayis, in *Rare-Earth Iron Permanent Magnets*, edited by J. M. D. Coey (Oxford University Press, Oxford, 1996).

¹³R. Skomski, *J. Appl. Phys.* **81**, 5627 (1997).

¹⁴H. Saito, M. Takahashi, T. Wakiyama, G. Kido, and H. Nakagawa, *J. Magn. Magn. Mater.* **82**, 322 (1989).

¹⁵R. Skomski, R. D. Kirby, and D. J. Sellmyer, *J. Appl. Phys.* **85**, 5069 (1999).

¹⁶M. Kersten, *Z. Phys.* **44**, 63 (1943).